

# Cutting Forces Prediction: the Experimental Identification of Orthogonal Cutting Coefficients

**Mihajlo Popovic**

University of Belgrade  
Faculty of Mechanical Engineering  
Production Engineering Department

**Ljubodrag Tanovic**

Full Professor  
University of Belgrade  
Faculty of Mechanical Engineering

**Kornel F. Ehmman**

Full time Professor  
Northwestern University  
Department of Mechanical Engineering  
Evanston, Illinois,  
USA

*In this paper the cutting coefficients were identified applying the orthogonal cutting mechanics, which are used in the cutting forces and torque prediction. The experiments were performed for material combination of the workpiece (16MnCr5) and tool (HSS-E, EMo5Co5). The first step in the forces prediction acting on a cutting tool is to consider a relatively simple orthogonal cutting process in order to continue to use the results of this analysis as a base for the development of a much more general case of oblique cutting. All cutting operations share the same cutting mechanics principles, but their geometry and kinematics are different. The accepted linear forces model includes both components, due to shearing and ploughing. The total forces are calculated based on the tool geometry by summing all active discretized cutting edges.*

**Keywords:** cutting forces prediction, cutting coefficients, orthogonal cutting mechanics, tool geometry

## 1. INTRODUCTION

The paper presents the procedure for the experimental identification of orthogonal cutting coefficients, which is a fundamental step in the cutting forces prediction.

Reliable prediction of cutting forces components in machining is of critical importance in the determination of the required power, dimensional accuracy, accuracy of form and surface roughness, vibrations and cutting tools and fixtures characteristics. The cutting force prediction is also needed in optimization strategies in the computer aided process planning (CAPP) and virtual machine systems [1-3]. The virtual machining represents the research direction that provides a response to the increasingly complex demands of modern industry such as the complexity of the product and the reduction of production time. Basically, virtual machining is near realistic computer simulation of machining process in the virtual world before its physical realization in the real world. The first goal of computer simulation is to provide insight into the effects of machining and its outputs for the projected part technology. This refers to the analysis of the cutting forces, where the need arises for the models of instantaneous cutting force, applicable for any tool geometry that will easily include new tool-workpiece material combination [1].

The forces that occur from the shear in primary and secondary cutting zone are included in the macro mechanical models. With such models, it is difficult to explain the different, often adverse effects that are manifested in real conditions at small uncut chip thickness.

In the research in the field of mechanics of the cutting, the effect at small thicknesses (sizing effect) is related to the processes of shearing and rubbing material in the tertiary cutting zone and to the appropriate components of the cutting force - edge or ploughing forces.

The accepted linear force model includes a component that derives from shear in the primary and secondary zone, which is proportional to the cross-section of the uncut chip thickness and phenomena that occur in the tertiary deformation zone, which is proportional to the width of cut and refers to edge forces.

Examples of the use of such models to forces prediction are shown in numerous research papers.

Kaymakci *et al.* [4] developed a unified cutting force model for turning, boring, drilling and milling operations with inserted tools.

The development and generic nature of the unified mechanics of cutting approach to technological performance prediction for a wide spectrum of machining operations is presented and discussed by Armarego [5]. Armarego and Herath [6] describe developed models for the force components, chip flow and power in turning of helical vee grooves as well as single pass turning at high and low feed to depth of cut ratios with triangular profiled form tools.

Force prediction in orthogonal cutting of unidirectional CFRP is reported by Qi *et al.* [7]. The force prediction in drilling of metal and composites is shown in papers [8-10]. The milling process is analyzed in papers [11-13], and the force prediction in thread milling is presented by Araujo *et al.* [14]. Models for prediction of tapping process were developed in papers [15-18].

Prediction of forces relies on experimental identification of cutting coefficients, found from a database, which usually contains values for a limited

Received: March 2016, Accepted: April 2016

Correspondence to: mr Mihajlo Popovic  
Faculty of Mechanical Engineering,  
Kraljice Marije 16, 11120 Belgrade 35, Serbia  
E-mail: mpopovic@mas.bg.ac.rs

doi: 10.5937/fmet1704459P

© Faculty of Mechanical Engineering, Belgrade. All rights reserved

FME Transactions (2017) 45, 459-467 459

number of tool and workpiece materials combinations [12, 14, 17]. For materials combinations not supported by a database, simple cutting experiments can provide necessary data [13, 18-22], while in the works [23-24] numerical simulations are used.

Numerical simulations of cutting process are based on finite element method (FEM) as a tool suitable for the cutting tool geometry and tool material optimization.

The experimental identification of cutting coefficients for accepted force model that describes cutting force components for a tool-workpiece material combination, specific cutting tool geometry and the cutting conditions, can be performed with methods relating to the three basic approaches: indirect - data obtained by experiments using specific types of processing, direct – general oblique cutting (mechanistic model) and hybrid – general orthogonal cutting with the orthogonal to oblique transformation (mechanics model). Instead of experiments in a real machine tools environment, the results of chip forming process obtained by the finite element method analysis can be used [23].

The goal of this paper is to present a methodology and set up measurement and data acquisition system for the identification of cutting coefficients applicable to all cutting processes, for a variety of tool-workpiece material combinations.

The content is structured as follows: Section 2 describes the accepted forces model. Section 3 describes the process of orthogonal cutting experiments. Section 4 includes the measurement results analysis and identification of orthogonal cutting coefficients.

## 2. THE FORCES MODEL

The general mechanics of workpiece material removal is explained by a simple case of orthogonal cutting. In orthogonal cutting, material is removed by the cutting edge perpendicular to the direction of the tool and workpiece relative movement. Mechanics of the most common cutting operations that are three-dimensional and geometrically complex (oblique cutting) are typically carried out by the geometrical and kinematics model of the transformation process applied to the orthogonal cutting [2].

Figure 1 shows the orthogonal cutting process basic elements. The layer of the material with cross-section  $a * b$ , is removed in the form of chips from the workpiece. The cutting forces acting in two perpendicular directions: main force  $F_1$  acts in the direction of cutting speed and radial force  $F_2$  acts perpendicularly to the machined surface.

Figure 2 shows cutting force vs. uncut chip thickness diagram, using the linear cutting force model. There are three deformation zones in the cutting process. This model includes the effects of all deformation zones which are related to (i) shearing, and (ii) friction, rubbing, ploughing and other dependencies.

Specific cutting forces,  $K_c$ , cover the plastic deformation in the shear plane during the chip formation. Edge force coefficients,  $K_e$ , cover other effects such as friction, rubbing, ploughing, and chip deformation [24].

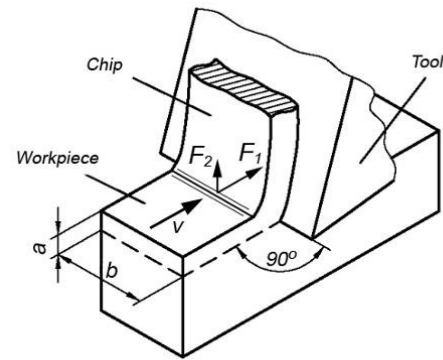


Figure 1. Orthogonal cutting geometry

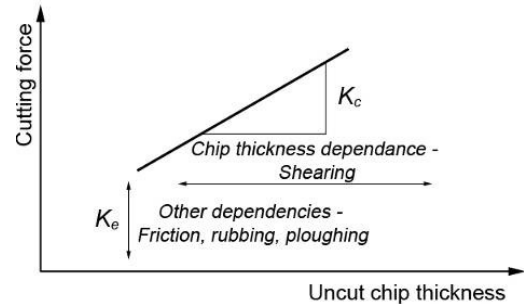


Figure 2. Mechanisms contributing to the cutting forces [24]

Figure 3 shows the cutting force diagram acting on the cutting wedge.

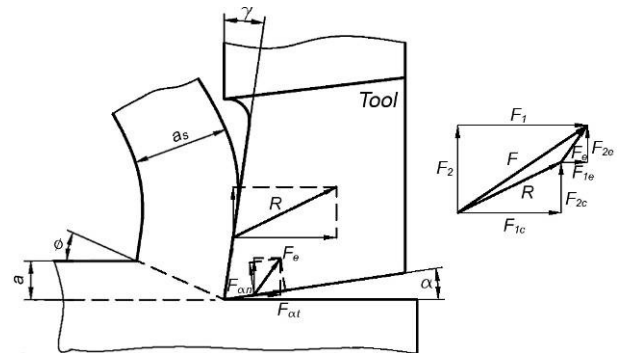


Figure 3. The forces involved in cutting, acting on the cutting wedge.

Cutting forces in a linear cutting model are typically expressed by shear ( $F_{1c}$ ,  $F_{2c}$ ) and flank contact ( $F_{1e}$ ,  $F_{2e}$ ) ploughing or edge components.

$$\begin{aligned} F_1 &= F_{1c} + F_{1e} = K_{1c}ab + K_{1e}b \\ F_2 &= F_{2c} + F_{2e} = K_{2c}ab + K_{2e}b \end{aligned} \quad (1)$$

where  $a$  is the uncut chip thickness,  $b$  width of cut, and  $K_i$  cutting force coefficients.

The hybrid method for experimental identification of orthogonal cutting coefficients that is independent of specific tool geometry was used in this paper. The data structures needed to identify the cutting coefficients is established through orthogonal cutting experiments in a series of turning tests. These cutting coefficients, with adequate general model for the orthogonal to oblique cutting transformation should enable calculation of the specific cutting forces for arbitrary cutting edge shape, with no restrictions in terms of the current orientation of such edges in relation to the cutting speed.

The forces that occur in the shear plane can be obtained from the forces balance on the chip, so the specific cutting forces  $K_c$  are:

$$K_{1c} = \tau_s \cdot \frac{\cos(\rho - \gamma_o)}{\sin \phi \cdot \cos(\phi + \rho - \gamma_o)} \quad (2)$$

$$K_{2c} = \tau_s \cdot \frac{\sin(\rho - \gamma_o)}{\sin \phi \cdot \cos(\phi + \rho - \gamma_o)} \quad (3)$$

where  $\tau_s$  is the shear stress

$$\tau_s = \frac{\sin \phi \cdot \cos(\phi + \rho - \gamma_o)}{a \cdot b} \cdot \sqrt{F_{1c}^2 + F_{2c}^2} \quad (4)$$

The angle  $\rho$  represents the average friction angle, and  $\gamma_o$  is the rake angle.

The shear plane angle,  $\phi$ , can be experimentally determined from the chip compression ratio, using equation:

$$\tan \phi = \frac{r_c \cdot \cos \gamma_o}{1 - r_c \cdot \sin \gamma_o} \quad (5)$$

The chip compression ratio,  $r_c$ , is given by:

$$r_c = \frac{a}{a_s} \quad (6)$$

where  $a_s$  is the chip thickness. For orthogonal cutting, the uncut chip thickness is equal to the feed rate ( $a=s$ ). The friction angle is given by:

$$\tan(\rho - \gamma_o) = \frac{F_{2c}}{F_{1c}} \Rightarrow \rho = \gamma_o + \arctan \frac{F_{2c}}{F_{1c}} \quad (7)$$

In the presented equations, the input data consists of the tool geometry – the rake angle and tool-workpiece material combination. Quantities to be identified are the shear stress, the friction angle, the shear angle and the chip compression ratio.

The  $K_{1c}$ ,  $K_{2c}$  are edge force coefficients in tangential and radial directions.

The edge forces are not part of the chip formation process, but are considered to be parasitic forces that occur as a result of the elastic response of the workpiece material on the tool rear surface (in the third deformation zone), assuming that the forces on the tool rake face have no influence [22].

Edge forces are difficult to isolate from the experimental data, however, significant efforts have been made to develop techniques for their identification. Different methods to reveal the edge forces are known from literature, such as the direct measurement method of the edge forces [20], the extrapolation method on zero uncut thickness [2, 21], and the comparison method of total forces at different flank wears [22].

The direct measurement method or zero feed method proposed monitoring force vs. time after cutting, but prior to the tool separation from the workpiece. The edge force is identified as the local maximum force of the first cycle of the cyclic force pattern.

The extrapolation method relies on the analysis of forces vs. uncut chip thickness graphic at a constant speed, and extrapolating on the zero uncut chip

thickness. In orthogonal cutting the uncut chip thickness is equal to feed rate.

The edge forces are particularly significant in the machining with smaller values of uncut chip thickness or in micro cutting, when they can be larger than the forces in the shear zone. These forces increase significantly with increasing of the cutting tool wear [22].

Based on experimentally determined cutting parameters and known cutting tool geometry, prediction procedure of the instant forces includes the following steps (Figure 4):

- (i) Cutting edge discretization using disks with elementary thickness,  $dz$ , to define elementary edges that can be considered linear. Elementary cutting force,  $dF$ , for every elementary edge fits the oblique cutting model.
- (ii) Identification of active elementary edges (in engagement with the workpiece) in the current position;
- (iii) The cutting forces calculation on active elementary edges.
- (iv) The predicted resultant cutting force components acting on the whole tool are obtained by numerical integration over all active elementary edges.

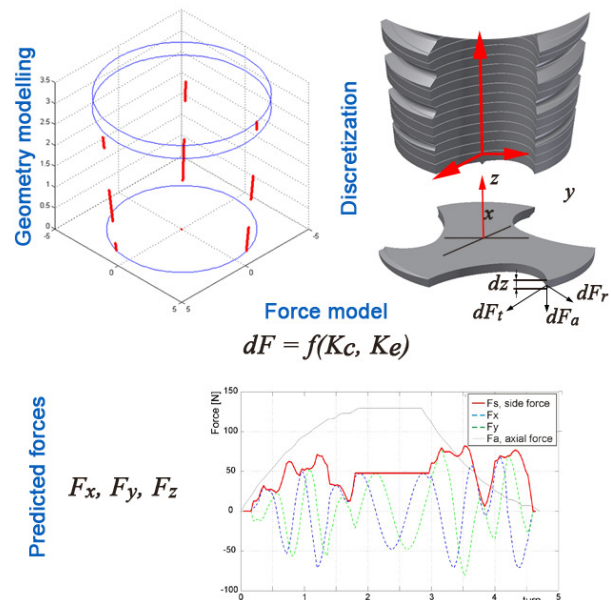


Figure 4. The cutting forces prediction procedure

Figure 4 shows the example of the cutting forces prediction procedure for threading tools – taps. Cutting tool geometry for the virtual manufacturing system is obtained from the CAD package. Cutting coefficients are experimentally determined for each tool-workpiece material combination.

### 3. ORTHOGONAL CUTTING EXPERIMENTS

For the procedure of experimental identification of cutting coefficients, which refers to a pair of HSS-E tool material and 16MnCr5 workpiece material in a limited range of cutting speeds, the hybrid method was used.

Any machining process requires a certain force to separate and remove the material, and researchers extensively use the measuring and monitoring of cutting forces for the validation of the proposed analytical process models, the detection of tool failure, etc. [26]

Orthogonal cutting can be done in two ways: longitudinally and transverse, Figure 5, and then only two cutting force components occurred. The feed motion direction coincides with the direction perpendicular to the machined surface. The depth of cut is equal to feed rate of an orthogonal turning process.

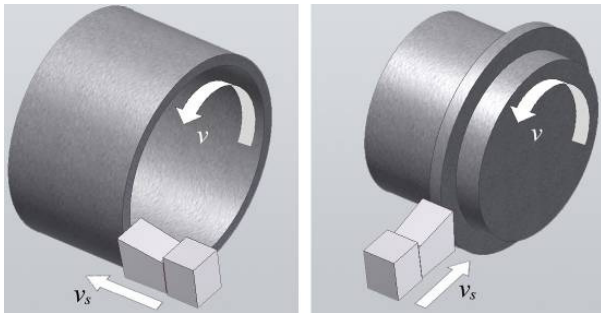


**Figure 5. Examples of orthogonal cutting in turning, longitudinal and transverse**

Figure 6 shows the model of machining and data acquisition system for cutting forces measurement during orthogonal cutting experiments on CNC turret lathe. Thus designed model is characterized by the following sections:

- CNC lathe machining system for orthogonal turning process;
- cutting forces sensor (two-component force dynamometer);
- inductive proximity sensor;
- amplifiers with power supply (signal conditioning);
- data acquisition module (A/D conversion, also has the ability of signal conditioning);
- personal computer with *Labview* software for data acquisition and control using the virtual instruments to enable the signal preview, backup, process and analysis.

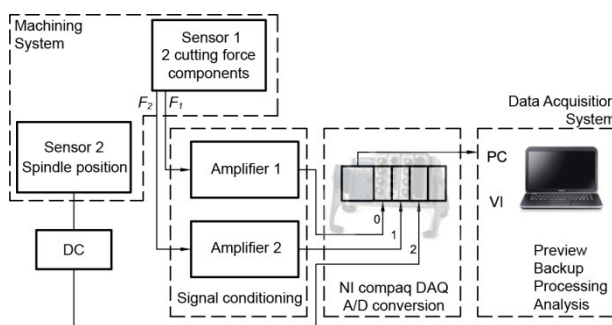


**Figure 6. The model of machining and data acquisition system for cutting forces measurement during orthogonal cutting experiments**

The experiments were performed at the Faculty of Mechanical Engineering in Belgrade: Machine Tools Institute, Department of Production Engineering, with the following stages of implementation:

- forming a plan of experiments,
- machining system preparation: POTISJE PH42 CNC turret lathe with the mounted dynamometer and tube blanks of 16MnCr5 steel material,
- data acquisition system installing and the dynamometer calibration, and
- conducting experiments according to the formed plan and chip marking and collection.

### 3.1 Experiment planning

Workpiece for experiments was a tube with an 80 mm outer diameter and 2.1 mm wall thickness. Workpiece material was a 16MnCr5 alloyed steel. The facing tools of different rake angles within the range of  $5 \div 20$  degrees are selected. Cutting speed ranges of  $10 \div 20$  m/min were used. Also, feed rates of  $0.01 \div 0.15$  mm/rev with small steps in cutting conditions were used to increase the measured forces reliability. These ranges meet all machining catches according to the recommended values for used tool-workpiece material combination [25].

Tool wear is controlled with a universal tool microscope in order to insure that it doesn't significantly influence the cutting forces.

### 3.2 CNC lathe machining system

Figure 7 presents the machining and acquisition systems applied to determine the forces in orthogonal cutting.



**Figure 7. Machining and data acquisition system**

In order to obtain the cutting coefficients necessary for the analysis presented in this work, facing tools were manufactured using the same HSS-E steel (EMo5Co5) as that used for machine taps serial production. Facing tools are designed and manufactured in  $8 \times 10 \times 100$  mm size, with four diverse rake angles ( $\gamma = 5^\circ, 10^\circ, 15^\circ$  and  $20^\circ$ ), and tool clearance of  $5^\circ$ . The tools had a sharp cutting edge.

Since the experiment uses the dynamometer which is not designed for special purposes, it was necessary to construct and produce a facing tool holder and a dynamometer holder for use on CNC turret lathe. Experiments were performed with cutting fluids switched off.

### 3.3 Data acquisition system

To measure the cutting forces, a custom made, two-component, strain gauge force dynamometer designed and made at Machine Tools Institute, amplifiers HBM KWS 3082A, NI CompactDAQ acquisition platform (NI USB 9174, NI 9215) and a laptop computer with *Windows 7* operating system and *LabVIEW* software for data acquisition were used.



## 4. MEASUREMENT RESULTS ANALYSIS

### a. Cutting forces

The typical cutting forces records into two perpendicular directions during the orthogonal turning process, with a holding tool in end cutting position are presented in Figure 8.

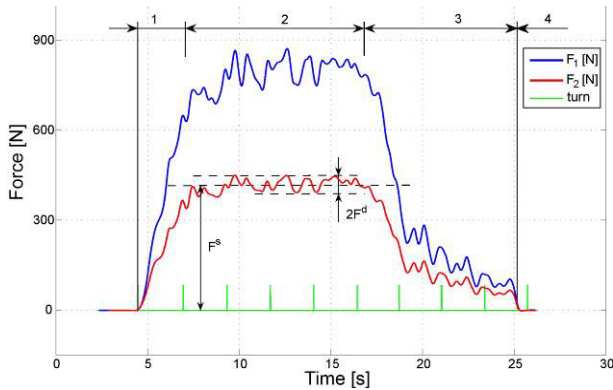


**Figure 8. Typical records of cutting forces as a function of time**

When cutting starts, the tool and the workpiece are in contact, cutting forces ( $F_1$ ,  $F_2$ ) begin to grow as the depth of cut increases to its maximum value which is equal to a given feed rate (zone 1) and continue to oscillate around a constant value in the further cutting process (zone 2). In this phase the dynamic character of cutting force is noticeable, which is reflected in the signal deviation from the mean - static force value. When tool reaches a specified length of cut, and it remains in the achieved position for some time (a few revolutions), cutting forces do not disappear but reduce to some finite values (zone 3) which are identified as edge forces [5, 6]. Only just in a moment of the tool returning to the starting point for the next catch, cutting forces disappear.

In order to shorten the time of conducting the experiment and thus minimize the tool wear, direct method for determining the value of the edge forces is applied in a limited number of experiments. The tool is held up at the cutting end point for ten seconds. Thus, only the existence of these forces is identified. The edge forces values are estimated by another method - the extrapolation method, and all other experiments were taken out without tool delay at the cutting end point.

The mean forces values and chips thickness were obtained for each of 150 experiments that have been performed with different rake angles, feed rates and cutting speeds. To calculate the mean cutting force value from steady-state phase of the experiment in the zone of constant depth of cut (zone 2) in Figure 8, the signal is averaged in the central 50% of this zone, as shown in Figure 9. In this way, the main forces and radial forces are obtained in all experiments.

Figure 10 shows one of the forces vs. uncut chip thickness diagram from orthogonal cutting test results, for cutting speed  $v = 10$  m/min and rake angle  $\gamma = 10^\circ$ .

For these cutting conditions the edge force coefficients are:

$$\begin{aligned} K_{1e} &= F_{1e}/b = 55.6/2.1 = 26.5 \text{ N/mm} \\ K_{2e} &= F_{2e}/b = 40.3/2.1 = 19.2 \text{ N/mm} \end{aligned} \quad (8)$$

while force components due to shearing are obtained from experimentally obtained total forces as:

$$\begin{aligned} F_{1c} &= F_1 - F_{1e} \\ F_{2c} &= F_2 - F_{2e} \end{aligned} \quad (9)$$

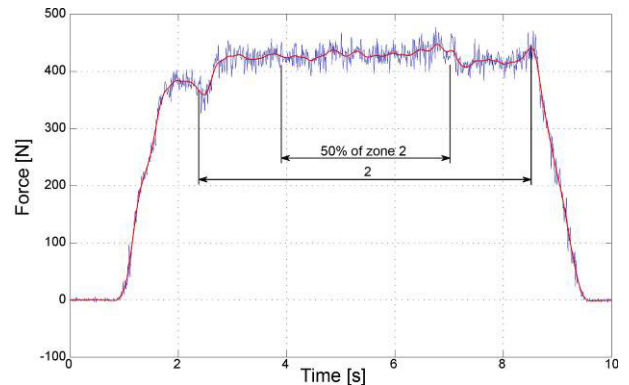


**Figure 9. Cutting force averaging**

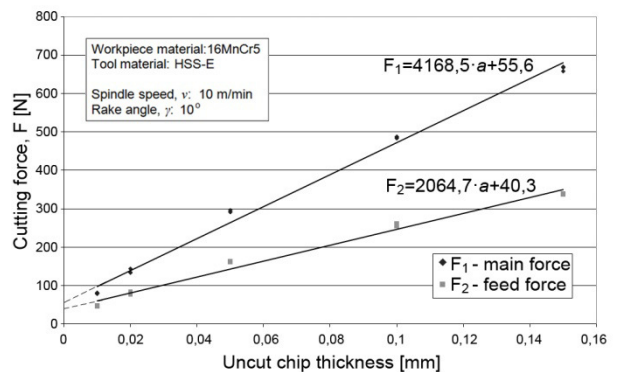


**Figure 10. Cutting forces as a function of uncut chip thickness ( $v=10$  m/min,  $\alpha=10^\circ$ )**

### b. The chip compression ratio determination

During the experiment, the chip samples are marked and collected for further analysis.

For experimental determination of the chip compression ratio there are several methods: measuring cutting velocity and chip velocity, volumetric, weighing and direct method for measuring the thickness. In addition, new methods that rely on the use of, now very affordable, high speed cameras and digital microscope cameras are proposed.

Volumetric and weighing method for the chip compression ratio determination are based on the equality of material volume before cutting and obtained chip volume. It is assumed that the material deformation in width direction is minimal.

To use the weighing method, it is necessary to determine workpiece material specific density,  $\rho_s$ , using the pycnometer, and measure the length,  $L_s$ , and mass,  $m_s$ , of the chip:

$$a_s = \frac{m_s}{b \cdot L_s \cdot \rho_s} \quad (10)$$

The collected chip samples were unbended and photos were taken with a digital microscope camera *dnt DigiMicro 2.0 Scale* (camera magnification up to 200 times; the resolution of 2 MP). These cameras are now

very affordable, have connection with a computer via USB port, and offer magnification up to 500 times and the ability to take photos with resolution up to 5 Megapixel.

Calibration of saved photos is performed through the calibrated plates for microscopes with a 0.01mm scale. The chip length is measured in the software that comes with the digital microscope camera, or in one of the vector drawing software that can easily follow the contour curves of measured object. Figure 11a shows a simple chip form which can be measured with a circular arc (the chip length is estimated as the mean length of the outer and inner contours). Figure 11b shows arbitrary chip form which is measured using splines in *AutoCAD* software. Thicker chips, which could not be unbend, were photographed in width on both sides, as shown in Figs 11c, d.

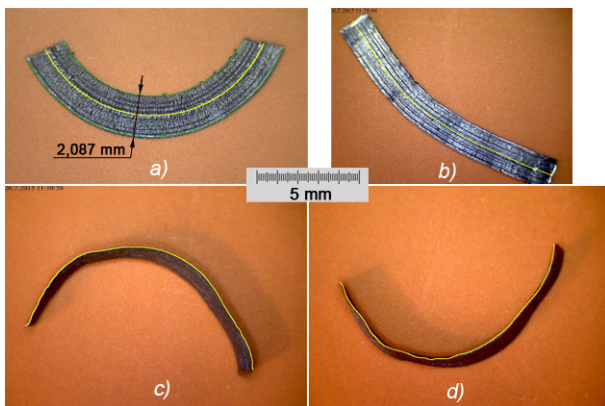


**Figure 11. Measuring the length of the chip samples**

Measurements of chips masses were made using electronic microbalance *Sartorius M 3 P-000V001* (*Sartorius GmbH, Weender Landstrasse, Germany*), Fig. 12, which is intended for samples measurement up to 1.5 g with an accuracy of 0.001mg. For example, the mass of chip with dimensions: 20mm length, 2.1mm width and 0.5mm thickness, for workpiece material specific density of  $7.85\text{mg}/\text{mm}^3$  is 165 mg.



**Figure 12. Electronic microbalance and chip samples**

In the direct method, the chip thickness can be measured using universal tools like vernier calipers, micrometers and thickness gauges with resolution 0.01mm or 0.001mm (digital). In order to increase the accuracy of the measured results, the measurement should be repeated in several places on a chip and works with average value. Measurement tools must have special measuring inserts and extensions for individual

customization (spherical, conical, arched or narrow surfaces) in order to reduce the influence of chip curvature.

Chip thickness ( $a_s$ ) measurement was undertaken with a point micrometer (range of 0-25 mm and resolution of  $10\ \mu\text{m}$ ), using 30 degree measuring points with 0.3 mm radius.

Photographic method uses a microscope or digital microscope camera, calibrated plates for microscopes and fixture for chips location and support. Chip thickness is estimated from the photography of chip cross-section. Figure 13 shows a chip cross-section obtained by digital microscope camera and marked chip thickness at multiple points in photo editing software after calibration.

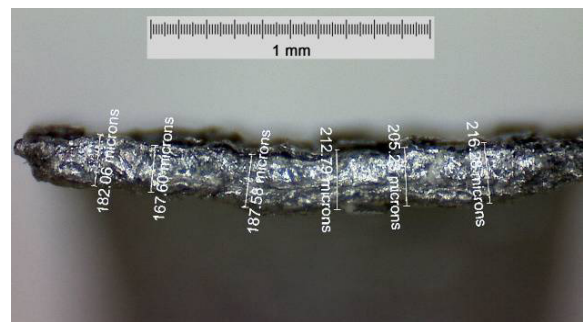


**Figure 13. Cross-section of chip thicknesses**

Photographing the cutting zone (Figure 14), or by recording with high speed camera (intended for slow motion playback), it is possible to identify the chip formation process during the cutting process. From the photo or video clip frame, the uncut chip thickness and chip thickness are determined in pixels and the chip compression ratio is calculated as their ratio.

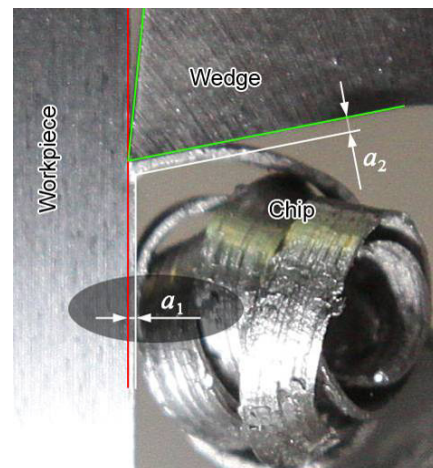


**Figure 14. Shear zone photo**

Each of these methods has its flaws that lead to inaccuracies in the determination of the chip thickness, and refer to: the problems determining the chip length at volumetric and weighing methods; focus point with the photographic and microscopic methods; contact of micrometer measuring points with the chip at direct method.

In this paper, the chip thickness is determined by a combination of weighing and direct methods compared with photographic method results in a limited number of experiments.

### c. Orthogonal cutting coefficients

Based on the measured cutting forces and chip thickness, results obtained from statistical analysis using the equation 2 - 7 of 150 orthogonal cutting experiments, lead to the unknown coefficients: the chip compression ratio, the shear angle, the average shear stress, the friction angle, and mean values for the edge force coefficients.

The shear stress,  $\tau_s$ , was simply averaged over data provided from orthogonal cutting experiments. The average friction angle,  $\rho$ , and chip compression ratio,  $r_c$ , were identified using statistical analysis of the same series of experimental data. Linear relationship properly describes the relationship between the average friction angle and the rake angle.

The dependence of the chip compression ratio on the uncut chip thickness and rake angle best describes the power function, where  $C_0$  is the scaling factor and  $C_1$  is the exponent. The chip ratio coefficients  $C_0$  and  $C_1$  are obtained in two steps, as linear relationship relative to the rake angle. Figure 15 shows the chip compression ratio relation  $r_{c(15)} = 0.781 a^{0.26}$  for the tool rake angle  $\gamma=15^\circ$ . The coefficients  $C_0$  and  $C_1$  as a function of the tool rake angle are presented in Figure 16.

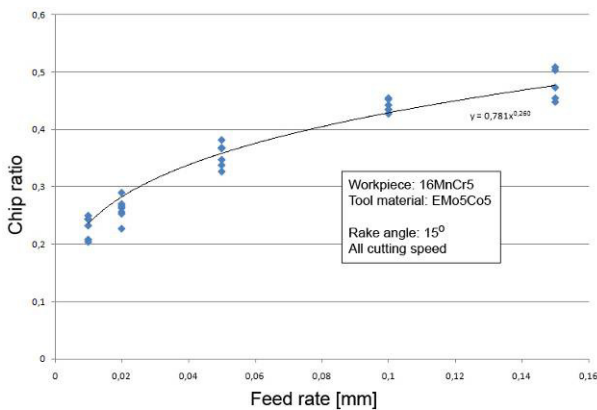


Figure 15. Chip compression ratio as a function of feed rate for  $\gamma=15^\circ$

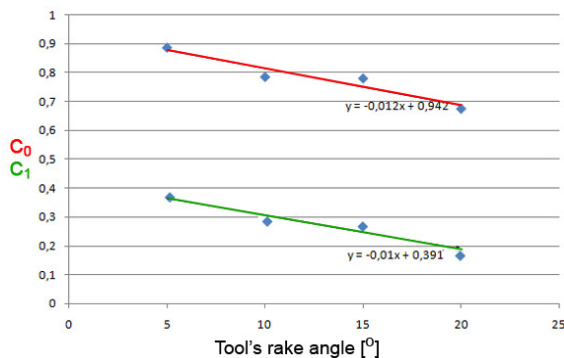


Figure 16. The chip ratio coefficients as a function of tool's rake angle

The mean values for edge force coefficients  $K_{1e}$  and  $K_{2e}$  were obtained by means of linear regression and extrapolation of measured forces to zero uncut chip thickness (Figure 10) and represent the edge forces per unit width [1, 4].

Cutting coefficients obtained for the material combination of tool (EMO5Co5) and workpiece (16MnCr5) are presented in Table 1.

Table 1. Orthogonal cutting coefficients data

$\tau_s = 558 \text{ MPa}$
$\rho = 35.18 + 0.627\gamma_o$
$r_c = C_0 a^{C_1}$ $C_0 = 0.942 - 0.012 \gamma_o$ $C_1 = 0.391 - 0.01 \gamma_o$
$K_{1e} = 28.8 \text{ N/mm}$
$K_{2e} = 21.5 \text{ N/mm}$

The following assumptions are made for using these parameters in oblique cutting: (i) shear angle in orthogonal cutting (equation 5) is equal to the normal shear angle in oblique cutting; (ii) the normal rake angle is equal to the rake angle in orthogonal cutting; (iii) the friction coefficient and shear stress are the same in both orthogonal and oblique cutting for given cutting conditions and tool-workpiece material combination.

### 5. CONCLUSION

The orthogonal cutting coefficients identification constitutes an important step in the instantaneous cutting force prediction, relating to all of deformation zones. The edge force is significantly important in tool wear monitoring, material flow stress calculation, chip formation mechanisms, and machined surface integrity.

The applied force model is applicable to all cutting processes, with adequate general model for the orthogonal to oblique cutting transformation on active elementary edges, taking into account the specific tool geometry, especially with new materials and coatings.

The novel methods for the experimental determination of the chip compression ratio are proposed. The experimentally provided cutting coefficients identified for applied tool and workpiece material combination and presented in Table 1, can be used to simulate any cutting process.

The established laboratory setup shall be used in the future for carrying out various tests and measurements, as well as comparison to the results of planned numerical simulations.

### REFERENCES

- [1] Altintas, Y., Brecher, C., Weck, M. and Witt, S.: Virtual Machine Tool, Cirp Ann-Manuf Technol, Vol. 54, No. 2, pp. 115-138, 2005.
- [2] Altintas, Y.: *Manufacturing Automation: Metal Cutting Mechanics, Machine Tool Vibrations, and CNC Design*, Cambridge University Press, Cambridge, UK, 2012.
- [3] Budak, E. et al.: Prediction of Milling Force Coefficients From Orthogonal Cutting Data, Journal of Manufacturing Science and Engineering, Vol. 118, pp. 216-224, 1996.
- [4] Kaymakci, M., Kilic, Z.M. and Altintas Y.: Unified cutting force model for turning, boring, drilling and milling operations, International Journal of Machine Tools & Manufacture, Vol. 54-55, pp. 34-45, 2012.
- [5] Armarego, E.J.A.: A Generic Mechanics of Cutting Approach to Predictive Technological Performance

Modeling of the Wide Spectrum of Machining Operations, *Machining Science and Technology*, Vol. 2, No. 2, pp. 191-211, 1998.

- [6] Armarego, E.J.A. and Herath, A.B.: Predictive Models for Machining with Multi-Edge Form Tools Based on a Generalised Cutting Approach, *Annals of the CIRP*, Vol. 49, No. 1, pp. 25-30, 2000.
- [7] Qi Z., Zhang K. et al.: Microscopic mechanism based force prediction in orthogonal cutting of unidirectional CFRP, *Int J Adv Manuf Technol*, Vol. 79, pp. 1209–1219, 2015.
- [8] Armarego, E.J.A. and Zhao, H.: Predictive Force Models for Point-Thinned and Circular Centre Edge Twist Drill Designs, *Annals of the CIRP*, Vol. 45, No. 1, pp. 65-70, 1996.
- [9] Yussefian N.Z. et al.: The prediction of cutting force for boring process, *International Journal of Machine Tools & Manufacture*, Vol. 48, pp. 1387–1394, 2008.
- [10] Lazar M.B. and Xirouchakis P.: Mechanical load distribution along the main cutting edges in drilling, *Journal of Materials Processing Technology*, Vol. 213, pp. 245–260, 2013.
- [11] Merdol, S.D. and Altintas, Y.: Virtual Simulation and Optimization of Milling Operations - Part I: Process Simulation, *Journal of Manufacturing Science and engineering*, Vol. 130, pp. 051004-1-12, 2008.
- [12] Moufki A., Dudzinski D. and Le Coz G.: Prediction of cutting forces from an analytical model of oblique cutting, application to peripheral milling of Ti-6Al-4V alloy, *The International Journal of Advanced Manufacturing Technology*, Vol. 81, No. 1, pp. 615-626, 2015.
- [13] Adem, K.A.M., Fales, R. and El-Gizawy A.S.: Identification of cutting force coefficients for the linear and nonlinear force models in end milling process using average forces and optimization technique methods, *Int J Adv Manuf Technol*, Vol. 79, No. 9-12, pp. 1671-1687, 2015.
- [14] Araujo, A.C., Silveira, J.L. and Kapoor, S.: Force prediction in thread milling, *J. Braz. Soc. Mech. Sci. & Eng.*, Vol. 26, No. 1, pp. 82-88, 2004.
- [15] Dogra A.P.S., Kapoor S.G. and DeVor R.E.: Mechanistic Model for Tapping Process With Emphasis on Process Faults and Hole Geometry, *Journal of Manufacturing Science and Engineering*, Vol. 124, pp. 18-25, 2002.
- [16] Cao, T. and Sutherland J.W.: Investigation of thread tapping load characteristics through mechanistics modeling and experimentation, *International Journal of Machine Tools & Manufacture*, Vol. 42, pp. 1527-1538, 2002.
- [17] Puzovic, R. and Kokotovic, B.: Prediction of thrust force and torque in tapping operations using computer simulation, *FME Transactions*, Vol. 34, No. 1, pp. 1-5, 2006.
- [18] Popovic, M. and Tanovic, Lj.: Tapping proces simulation based on orthogonal cutting tests, in: *Proceedings of the II International scientific*

*conference COMETA*, 02-05.12.2014, Jahorina, pp. 25-32.

- [19] Gao G., Wu B., Zhang D. and Luo M.: Mechanistic identification of cutting force coefficients in bull-nose milling process, *Chinese Journal of Aeronautics*, Vol. 26, No. 3, pp. 823–830, 2013.
- [20] Stevenson, R.: The measurement of parasitic forces in orthogonal cutting, *Int. J. Mach. Tools Manufact.*, Vol. 38, pp. 113-130, 1998.
- [21] Guo, Y.B. and Chou, Y.K.: The determination of ploughing force and its influence on material properties in metal cutting, *Journal of Materials Processing Technology*, Vol. 148, pp. 368-375, 2004.
- [22] Popov A. and Dugin A.: Effect of uncut chip thickness on the ploughing force in orthogonal cutting, *Int J Adv Manuf Technol*, Vol. 76, pp. 1937-1945, 2015.
- [23] Gonzalo O., Jauregi H., Uriarte L.G. and Lopez de Lacalle L.N.: Prediction of specific force coefficients from a FEM cutting model, *International Journal of Advanced Manufacturing Technology*, Vol. 43, pp. 348–356, 2009.
- [24] Gonzalo O., Beristain J., Jauregi H. and Sanz C.: A method for the identification of the specific force coefficients for mechanistic milling simulation, *International Journal of Machine Tools & Manufacture*, Vol. 50, pp. 765–774, 2010.
- [25] Kalajdzic, M., et al.: *The machining technology – Handbook* (in serbian), University of Belgrade, Faculty of Mechanical Engineering, Belgrade, 2012.
- [26] Teti, R., Jemielniak, K., O'Donnell, G. and Dornfeld, D.: Advanced monitoring of machining operations, *CIRP Annals - Manufacturing Technology*, Vol. 59, pp. 717–739, 2010.

## NOMENCLATURE

$a$	uncut chip thickness, mm
$a_s$	chip thickness, mm
$b$	edge width, mm
$C_0, C_1$	coefficients
$F_1$	main cutting force, N
$F_2$	feed cutting force, N
$K_{1c}, K_{2c}$	specific cutting forces, N/mm <sup>2</sup>
$K_{1e}, K_{2e}$	edge force coefficients, N/mm
$L_s$	chip length, mm
$m_s$	chip mass, mg
$r_c$	chip compression ratio
$s$	feed rate, mm/rev
$v$	cutting speed, m/min
$z$	thickness, mm

## Greek symbols

$\alpha$	tool clearance, °
$\gamma_0$	rake angle, °
$\rho$	friction angle, °
$\rho_s$	specific density, mg/mm <sup>3</sup>
$\phi$	shear plane angle, °
$\tau_s$	shear stress, N/mm <sup>2</sup>



*Superscripts*

c	cutting force
e	edge force

---

**ПРЕДИКЦИЈА СИЛА РЕЗАЊА:  
ЕКСПЕРИМЕНТАЛНА ИДЕНТИФИКАЦИЈА  
ПАРАМЕТАРА ОРТОГОНАЛНОГ РЕЗАЊА**

**М. Поповић, Љ. Тановић, К. Ehmann**

У раду је приказана процедура за одређивање скупа параметара резања тестовима ортогоналног стру-

гања који се користи за предикцију сила и момента резања. Експерименти су извођени за комбинацију материјала обратка (С4320) и резног алата (С9780). Први корак у предикцији сила се односи на разматрање релативно једноставног процеса ортогоналног резања, да би се резултати анализе даље користили као основа за развој много општијег случаја косог резања. Све операције резања деле исте принципе механике резања, али њихова геометрија и кинематика се разликују. Усвојени линеарни модел силе укључује силе услед смицања и ивичне силе. Укупна сила се одређује на основу конкретне геометрије алата сумирањем по свим активним елементарним сечивима.